Tetrahedron Letters 50 (2009) 6909–6912

Contents lists available at ScienceDirect

Tetrahedron Letters

journal homepage: www.elsevier.com/locate/tetlet

Linear fully conjugated *meso*-aryl pentapyrrins

Ji-Young Shin, Steven S. Hepperle, David Dolphin *

Department of Chemistry, University of British Columbia, 2036 Main Mall, Vancouver, BC, Canada V6T 1Z1

ARTICLE INFO

Article history:
Received 27 August 2009
Revised 23 September 2009
Accepted 24 September 2009
Available online 29 September 2009

ABSTRACT

A *meso*-2,6-dichlorophenyl pentapyrrin was prepared using a modified method for dipyrrane synthesis followed by simple DDQ oxidation. The fully conjugated structures formed via redox inter-conversions were studied using crystallographic as well as observed and calculated spectral data.

meso-Substituted polypyrranes have become important precursors for the synthesis of *meso*-substituted expanded, contracted, and isomeric porphyrins.[1–3] Synthetic pathways to these compounds have been well established.[4] A one-flask synthesis of dipyrromethanes was introduced, primarily, by Lindsey's group[4] and developed to achieve the synthesis of multigram quantities of dipyrromethanes via simple purification methods.[5] Utilizing a modified synthetic method,[6] Lee's group have prepared *meso*-substituted tripyrromethanes, as the major component, along with other products such as dipyrromethanes and larger polypyrromethanes. A previously reported synthetic method for tripyrromethanes[7] was employed in our recent research to prepare polypyrromethanes ranging from tripyrromethanes to heptapyrromethanes.[8]

Since the oxidation of *meso*-aryl tripyrromethanes can result in the formation of macrocyclic compounds[4] and tripyrrinone isomers,[8] we were also interested in the oxidations of relatively higher polypyrromethanes. Gross and his colleagues reported the formation of a *meso*-aryl pentapyrrin from a solvent-free condensation reaction of pyrrole and pentafluorobenzaldehyde.[9] The aromaticity of macrocyclic compounds such as porphyrins and expanded porphyrins have been extensively studied during the last decade,[10–15] while linear oligopyrroles, having a continuous π-conjugated network, have been less well understood due to their flexibility and consequent lack of control of their configurations. The aromaticity of conjugated macrocyclic compounds has been widely studied and here we discuss the aromaticity of open-chain compounds.

Fortunately, single crystals of a 2,6-dichlorophenyl-substituted pentapyrrin having three amino-Ns in its molecular skeleton were successfully grown and the crystal structure of **1** (Fig. 1) represents one of three possible oxidation states that retains a conjugated network along the main skeleton as shown in Scheme 1. Using the initial crystallographic data, the other oxidation states containing different conjugation networks were geometrically-optimized by DFT calculation.

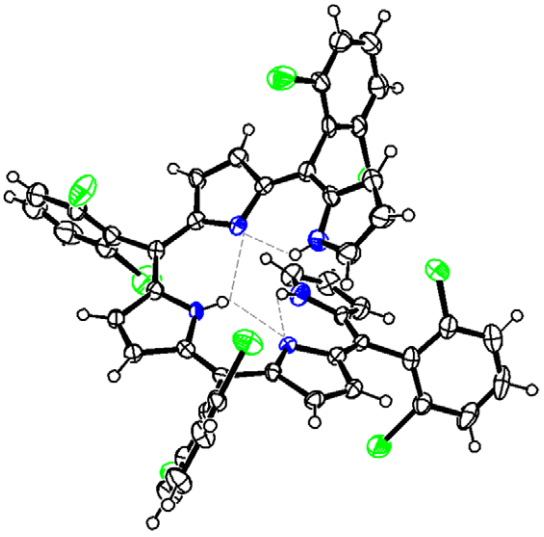

Figure 1. Crystal structure of **1**;[16] intramolecular hydrogen-bonds are denoted by dashed lines.

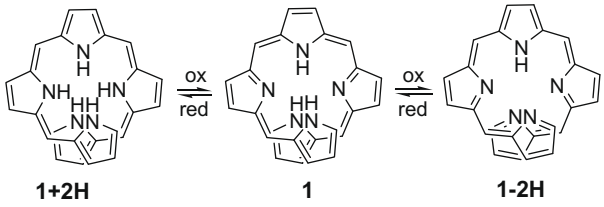

Scheme 1. Three possible forms of a pentapyrrin showing various oxidation levels.

A series of *meso*-2,6-dichlorophenyl oligopyrroles was prepared from pyrrole, dipyrromethane, and arylaldehydes by acid-

* Corresponding author. Tel.: +1 604 822 4571; fax: +1 604 822 9678.
E-mail address: david.dolphin@ubc.ca (D. Dolphin).

0040-4039/$ - see front matter © 2009 Elsevier Ltd. All rights reserved.
doi:10.1016/j.tetlet.2009.09.145

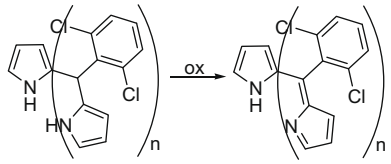

Scheme 2. *meso*-2,6-Dichlorophenyl polypyrromethanes and polypyrrins.

catalyzed condensation using TFA (see the Supplementary data and Scheme 2), and oxidized to from fully conjugated linear oligomers. Based on the NMR data for tetrapyrrin, pentapyrrin, and hexapyrrin, the molecular structures are delocalized symmetric compounds stabilized by intramolecular hydrogen-bonding. As a result, only half the expected number of hydrogen signals was observed in the spectra. Here, we focus on the structural and spectral properties of the pentapyrrins.

A single crystal of 2,6-dichlorophenyl-substituted pentapyrrin (**1**) was obtained by vapor diffusion of hexane into a CH_2Cl_2 solution. The structure was determined by X-ray diffraction analysis as shown in Figure 1. Similar to the crystal structure of *meso*-perfluorophenyl pentapyrrin reported by Gross and co-workers the crystal structure of *meso*-1,6-dichlorophenylpentapyrrin exhibits a helical structure made more rigid by intramolecular hydrogen-bonds between the imino-Ns and amino-NHs (Fig. 1). The NH peak was observed at 12.59 nm which is considerably downfield due to the intramolecular hydrogen-bond formation. The NMR data confirms the symmetry of the molecule. As noted above, the pentapyrrin can exist in three different π-conjugated networks as shown in Scheme 1. The most stable form of the pentapyrrin can be expected as **1** due to the nature of the intramolecular hydrogen-bonds as revealed by the single crystal analysis.

The optical spectrum of a CH_2Cl_2 solution gradually changed upon the addition of DDQ (Fig. 2). B-like bands were hypsochromically-shifted while the Q-like bands appeared over a broad range (700–1000 nm) with bathochromic shifts. This B-like band shift in the observed optical spectrum was also confirmed in the calculated optical spectrum[17,18] (Fig. 3). Reduction of **1**, in acetone, using $NaBH_4$ gave the changes shown in Figure 4. The desired product **1+2H** is unstable due, presumably, to the lack of any internal hydrogen-bonding. As shown in the photograph in Figure 4, the reddish-pink solution (**1+2H**) after reduction of **1** returned to the original orange color of **1** once the excess borohydride was removed.

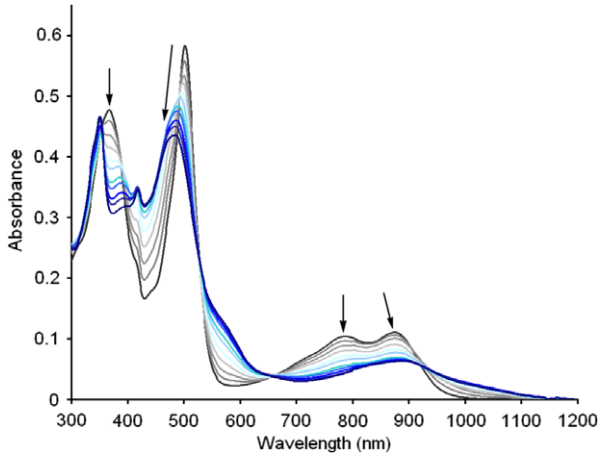

Figure 2. Optical spectral changes of **1** in following progressive oxidation; the dark blue line is the final spectrum.

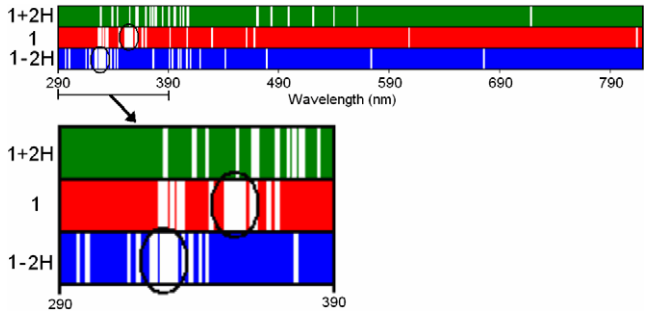

Figure 3. Optical spectral dependence of **1** relative to the oxidation level; these theoretical spectra were obtained by DFT calculations.

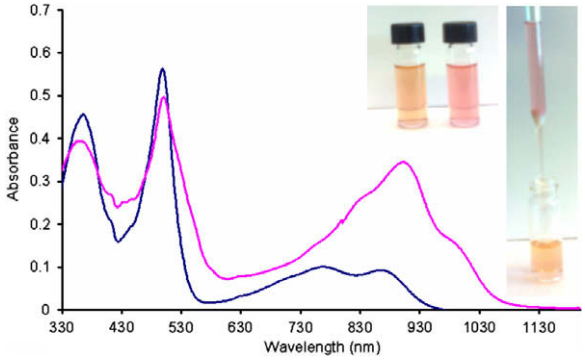

Figure 4. Optical spectral changes observed upon the reduction of **1** using $NaBH_4$: before (dark blue line) and after (purple line) addition. The color of the solution changed to the original orange after removal of excess borohydride by filtration and standing open to the air.

The geometrically-optimized structures shown in Figure 5 were obtained by Gaussian calculations.[17,19] Compared to the structure of **1+2H** where all Ns are protonated, the structures of **1** and **1-2H** having imino-Ns showed a more compact configuration due to the intramolecular hydrogen-bonding, with **1** being the most compact. As shown in Figure 6, the dihedral angles for each compound were determined as 82.9°, 43.1°, and 48.5° for **1+2H**, **1,** and **1-2H**, respectively, and **1** was thus considered to be the most stable form. Also, relatively, **1** exhibits the smallest dihedral angle between the mean planes for both of the dipyrrins attached to the middle pyrrole ring (Fig. 6). Typical N–H···N hydrogen-bond strengths are 13 kJ/mol. Molecule **1** is expected to have an additional stability of roughly 26 kJ/mol as it possesses two more NH–N intramolecular hydrogen-bonds than **1-2H**. Compound **1+2H** has no such additional stability.

NMR data of **1** and **1+2H** were obtained by DFT calculation.[17,20] The results for **1** are very consistent with the observed NMR data (Fig. 7, Table 1). On the other hand, it was thought that the increase in flexibility for **1+2H**, due to the absence of intramolecular hydrogen-bonds, would alter the chemical shift magnitude in NMR. While the values of the observed and calculated data for **1** are 56.8 and 52.0 ppm for ^{13}C and 6.7 and 6.6 ppm for ^{1}H, respectively, the values on the calculated data for **1+2H** are 41.1 ppm and 2.4 ppm for ^{13}C and ^{1}H, respectively.

Macrocyclic compounds containing continuous π-conjugated networks have been widely studied with respect to their magnetic properties. We have here reported how changes in conjugation networks in open-chain fully conjugated molecules influence their overall geometry and molecular properties.

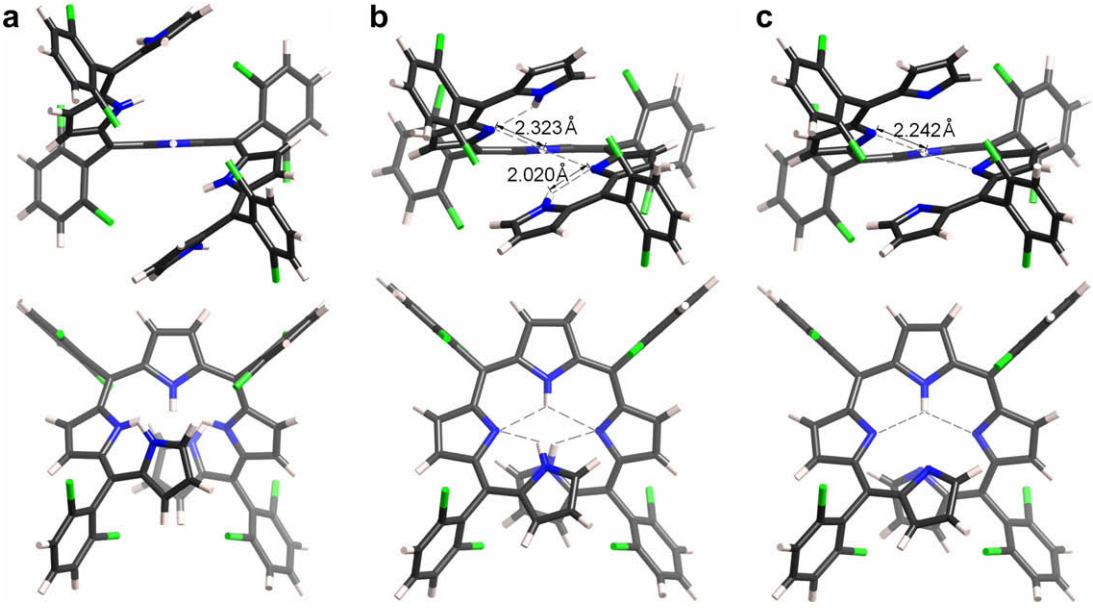

Figure 5. Geometry of the optimized structures of pentapyrrins (a) **1+2H**, (b) **1** and (c) **1-2H**.

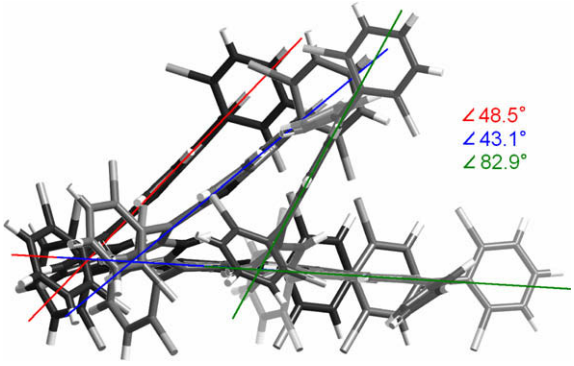

Figure 6. Dihedral angles between two dipyrromethene mean planes attached to the middle pyrrole ring of 1-2H, 1, and 1+2H.

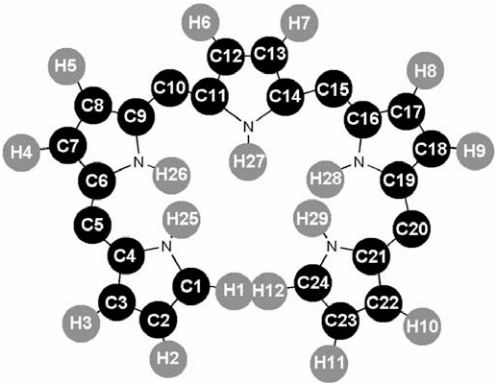

Figure 7. Atomic labels for the NMR data.

Table 1
NMR data comparison for compound **1**

Label	Observed		Calculated[19]		
	1-2H	**1**	**1-2H**	**1**	**1+2H**
C1, C24	–	131.67	165.10	127.81	117.36
C2, C23	–	112.47	127.24	110.69	109.25
C3, C22	–	119.41	133.34	118.32	108.39
C4, C21	–	133.69	157.52	134.04	131.85
C5, C20	–	130.33	136.61	133.17	104.95
C6, C19	–	152.23	165.50	153.20	122.65
C7, C18	–	134.97	128.14	131.11	124.15
C8, C17	–	126.51	131.17	123.47	122.65
C9, C16	–	166.60	154.92	162.65	142.24
C10, C15	–	109.83	139.14	112.69	101.10
C11, C14	–	147.75	142.13	145.39	130.23
C12, C13	–	129.01	122.01	125.91	111.60
H1, H12	6.51	6.50	7.79	7.06	7.19
H2, H11	6.08	6.08	6.63	6.55	6.69
H3, H10	5.90	5.89	6.78	6.22	6.08
H4, H9	6.47	6.48	6.62	6.82	6.10
H5, H8	6.23	6.22	6.85	6.29	6.05
H6, H7	6.36	6.36	6.76	6.55	6.21
H25, H29	–	12.59	–	12.84	8.40
H26, H28	–	–	–	–	7.85
H27	12.9	12.59	12.97	11.79	8.45

Research into further understanding the structural interconversion of pentapyrrins and their diverse π-conjugated forms as well as investigation into other polypyrrins is underway.

Acknowledgments

This work was supported by the Natural Sciences and Engineering Research Council (NSERC) of Canada. We thank Dr. Brian Patrick of the UBC Department of Chemistry for the single crystal diffraction analysis.

Supplementary data

Supplementary data (NMR spectra of the compounds and crystallographic (cif) and DFT calculation data) associated with this article can be found, in the online version, at doi:10.1016/j.tetlet.2009.09.145.

References and notes

1. Lindsey, J. S. *Metalloporphyrin Catalyzed Oxidations*; Kluwer Academic Press: The Netherlands, 1994. pp 49–86 and references therein.
2. Wagner, R. W.; Johnson, T. E.; Lindsey, J. S. *J. Am. Chem. Soc.* **1996**, *118*, 11166–11180.
3. *Expanded, Contracted & Isomeric Porphyrins*; Sessler, J. L., Weghorn, S. J., Eds.; Pergamon: Oxford, 1997; Jasat, A.; Dolphin, D. *Chem. Rev.* **1997**, *97*, 2267–2340.
4. Lee, C.-H.; Lindsey, J. S. *Tetrahedron* **1994**, *50*, 11427–11440.
5. Littler, B. J.; Miller, M. A.; Hung, C. H.; Wagner, R. W.; O'Shea, D. F.; Boyle, P. D.; Lindsey, J. S. *J. Org. Chem.* **1999**, *64*, 1391–1396; Laha, J. K.; Dhanalekshmi, S.; Taniguchi, M.; Ambroise, A.; Lindsey, J. S. *Org. Process Res. Dev.* **2003**, *7*, 799–812.
6. Ka, J.-W.; Lee, C.-H. *Tetrahedron Lett.* **2000**, *41*, 4609–4613; Brückner, C.; Sternberg, E. D.; Boyle, S. R.; Dolphin, D. *Chem. Commun.* **1997**, 1689–1690.
7. Taniguchi, R.; Shimizu, S.; Suzuki, M.; Shin, J.-Y.; Furuta, H.; Osuka, A. *Tetrahedron Lett.* **2003**, *44*, 2505–2507.
8. Shin, J.-Y.; Hepperle, S. S.; Patrick, B. O.; Dolphin, D. *Chem. Commun.* **2009**, 2323–2325.
9. Gross, Z.; Galili, N.; Simkhovich, L.; Saltsman, I.; Botoshansky, M.; Bläser, D.; Boese, R.; Goldberg, I. *Org. Lett.* **1999**, *1*, 599.
10. Shimizu, S.; Taniguchi, R.; Osuka, A. *Angew. Chem., Int. Ed.* **2005**, *44*, 2225–2229.
11. Shin, J.-Y.; Furuta, H.; Osuka, A. *Angew. Chem., Int. Ed.* **2001**, *40*, 619–621.
12. Shin, J.-Y.; Furuta, H.; Yoza, K.; Igarashi, S.; Osuka, A. *J. Am. Chem. Soc.* **2001**, *123*, 7190–7191.
13. Park, J. K.; Yoon, Z. S.; Yoon, M. C.; Kim, K. S.; Mori, S.; Shin, J.-Y.; Osuka, A.; Kim, D. *J. Am. Chem. Soc.* **2008**, *130*, 1824–1825.
14. Richter, D. T.; Lash, T. D. *Tetrahedron* **2001**, *57*, 3657–3671.
15. Pacholska-Dudziak, E.; Skonieczny, J.; Pawlicki, M.; Szterenberg, L.; Ciunik, Z.; Latos-Grażyński, L. *J. Am. Chem. Soc.* **2008**, *130*, 6182–6185.
16. CCDC 745166; see the Supplementary data.
17. Frisch, M. J.; Trucks, G. W.; Schlegel, H. B.; Scuseria, G. E.; Robb, M. A.; Cheeseman, J. R.; Montgomery, Jr., J. A.; Vreven, T.; Kudin, K. N.; Burant, J. C.; Millam, J. M.; Iyengar, S. S.; Tomasi, J.; Barone, V.; Mennucci, B.; Cossi, M.; Scalmani, G.; Rega, N.; Petersson, G. A.; Nakatsuji, H.; Hada, M.; Ehara, M.; Toyota, K.; Fukuda, R.; Hasegawa, J.; Ishida, M.; Nakajima, T.; Honda, Y.; Kitao, O.; Nakai, H.; Klene, M.; Li, X.; Knox, J. E.; Hratchian, H. P.; Cross, J. B.; Bakken, V.; Adamo, C.; Jaramillo, J.; Gomperts, R.; Stratmann, R. E.; Yazyev, O.; Austin, A. J.; Cammi, R.; Pomelli, C.; Ochterski, J. W.; Ayala, P. Y.; Morokuma, K.; Voth, G. A.; Salvador, P.; Dannenberg, J. J.; Zakrzewski, V. G.; Dapprich, S.; Daniels, A. D.; Strain, M. C.; Farkas, O.; Malick, D. K.; Rabuck, A. D.; Raghavachari, K.; Foresman, J. B.; Ortiz, J. V.; Cui, Q.; Baboul, A. G.; Clifford, S.; Cioslowski, J.; Stefanov, B. B.; Liu, G.; Liashenko, A.; Piskorz, P.; Komaromi, I..; Martin, R. L.; Fox, D. J.; Keith, T.; Al-Laham, M. A.; Peng, C. Y.; Nanayakkara, A.; Challacombe, M.; Gill, P. M. W.; Johnson, B.; Chen, W.; Wong, M. W.; Gonzalez, C.; Pople, J. A. GAUSSIAN *03, Revision E.01*; Gaussian: Wallingford, CT, 2007.
18. Time-dependent density functional theory (TDDFT) with B3LYP was utilized to calculate the optical spectra: Runge, E.; Gross, E. K. U. *Phys. Rev. Lett.* **1984**, *52*, 997–1000; Gross, E. K. U.; Kohn, W. *Phys. Rev. Lett.* **1985**, *55*, 2850–2852.
19. Geometry optimizations were performed using the Kohn-Sham method B3LYP with Pople's 6-31G(d,p) basis set. Solvent effects were considered by employing an integral equation formalism polarizable continuum model (PCM) appropriate for methylene chloride with the MP2 energies: Becke, A. D. *J. Chem. Phys.* **1993**, *98*, 5648–5652; Lee, C.; Yang, W.; Parr, R. G. *Phys. Rev. B* **1988**, *37*, 785–789; Hariharan, P. C.; Pople, J. A. *Theor. Chim. Acta* **1973**, *28*, 213–222; Francl, M. M. W.; Pietro, J.; Hehre, W. J.; Binkley, J. S.; DeFrees, D. J.; Pople, J. A.; Gordon, M. S. *J. Chem. Phys.* **1982**, *77*, 3654–3665; Hehre, W. J.; Ditchfield, R.; Pople, J. A. *J. Chem. Phys.* **1972**, *56*, 2257–2261; Mennucci, B.; Tomasi, J. *J. Chem. Phys.* **1997**, *106*, 5151–5158; Cancès, E.; Mennucci, B.; Tomasi, J. *J. Chem. Phys.* **1997**, *107*, 3032–3041; Mennucci, B.; Cancès, E.; Tomasi, J. *J. Phys. Chem. B* **1997**, *101*, 10506–10517; Tomasi, J.; Mennucci, B.; Cancès, E. *THEOCHEM* **1999**, *464*, 211–226.
20. The ^{1}H and ^{13}C NMR chemical shifts for the molecules were calculated with the gauge-independent atomic orbital (GIAO) method at the B3LYP/6-31+G(df,p) level of theory (with PCM solvent effects) using the B3LYP/6-31G** optimized geometries: London, F. *J. Phys. Radium.* **1937**, *8*, 397–409; McWeeny, R. *Phys. Rev.* **1959**, *114*, 1528–1529; Ditchfield, R. *Mol. Phys.* **1974**, *27*, 789–807; Dodds, J. L.; McWeeny, R.; Sadlej, A. J. *Mol. Phys.* **1977**, *34*, 1779–1791; Wolinski, K.; Hinton, J. F.; Pulay, P. *J. Am. Chem. Soc.* **1990**, *112*, 8251–8260.